884 Laser Physics Letters Laser Phys. Lett. **4**, No. 12, 884–889 (2007) / **DOI** 10.1002/lapl.200710075

Abstract: Multiple Stokes and anti-Stokes generation in the monoclinic tungstate $MnWO_4$ was observed under one-micron picosecond excitation. All the recorded Raman induced laser lines were identified and attributed to the SRS-promoted vibration mode (at $\approx 879\ cm^{-1}$) of the crystal.

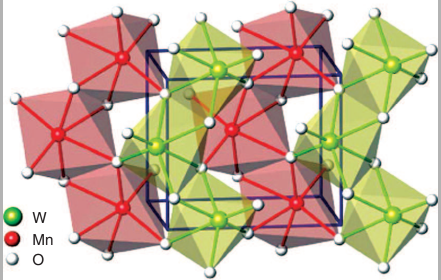

Section of the crystal structure of $MnWO_4$

High-gain Raman induced multiple Stokes and anti-Stokes generation in monoclinic multiferroic $MnWO_4$ single crystals

P. Becker, [1] *L. Bohatý,* [1] *H.J. Eichler,* [2] *H. Rhee,* [2] *and A.A. Kaminskii* [3,*]

[1] Institute of Crystallography, University of Cologne, 50674 Cologne, Germany
[2] Institute of Optics and Atomic Physics, Technical University of Berlin, 10623 Berlin, Germany
[3] Institute of Crystallography, Russian Academy of Sciences, 59, Leninskii pr., Moscow 119333, Russia

Received: 28 July 2007, Accepted: 31 July 2007

Key words: stimulated Raman scattering; Stokes and anti-Stokes generation; Raman laser shifter; multiferroic crystal; $MnWO_4$

PACS: 42.55.Rz, 42.65.Dr, 42.70.-a, 78.30.-j

1. Introduction

Numerous tungstates with complex anions, undoped or doped with trivalent lanthanides (Ln^{3+}) or transition metal lasants (only Cr^{3+} so far), have been playing an important role in modern quantum electronics and nonlinear optics for about almost fifty years [1]. Their crystal-chemical diversity provides crystals with a wide variety of physical properties. From a historical point of view it is interesting to note here that the tetragonal calcium tungstate Nd^{3+}:$CaWO_4$ was the first laser crystal doped with lanthanide ions Ln^{3+} [2]. In addition to their known laser potential, tungstate crystals with ordered or disordered structure also have $\chi^{(3)}$ nonlinearity that makes them attractive for stimulated Raman scattering (SRS), see Table 1. Combined with stimulated emission (SE) this nonlinearity allows to develop new sources of laser radiation that can enrich the spectral diversity of crystalline lasers. Therefore, the investigation of optical properties (based on $\chi^{(3)}$ nonlinearity) of further crystals of the tungstate family is of currently burning interest. In this work, we report on the first observation of Raman induced Stokes and anti-Stokes generation in undoped monoclinic single crystals of manganese tungstate, $MnWO_4$.

2. Crystallography of $MnWO_4$

Manganese tungstate $MnWO_4$ is known as a mineral species named *huebnerite* since 1865 [5]. An early struc-

---

[*] Corresponding author: e-mail: kaminalex@mail.ru

Crystal	Space group	Lasing ion	Observed nonlinear laser effect	SRS-active vibration modes, cm^{-1}
NaY(WO$_4$)$_2$	$C_{4h}^6 - I4_1/a$	Nd^{3+}	SRS	$\approx$914, $\approx$328
NaLa(WO$_4$)$_2$	$C_{4h}^6 - I4_1/a$	Nd^{3+}	SRS$^{a)}$	$\approx$900
Na$_5$Nd(WO$_4$)$_4$	$C_{4h}^6 - I4_1/a$	Nd^{3+}	-	-
NaGd(WO$_4$)$_2$	$C_{4h}^6 - I4_1/a$	Nd^{3+}, Tm^{3+}, Yb^{3+}	SRS $^{a)}$	$\approx$900
NaLu(WO$_4$)$_2$	$C_{4h}^6 - I4_1/a$	Yb^{3+}	-	-
NaBi(WO$_4$)$_2$	$C_{4h}^6 - I4_1/a$ $^{b)}$	Nd^{3+}	SRS	$\approx$910
Al$_2$(WO$_4$)$_3$	$D_{2h}^{14} - Pbcn$	Cr^{3+}	-	-
α-KY(WO$_4$)$_2$	$C_{2h}^6 - C2/c$	Pr^{3+}, Nd^{3+}, Dy^{3+}, Ho^{3+}, Er^{3+}, Tm^{3+}, Yb^{3+}	SRS, self-SRS (Nd^{3+}, Yb^{3+}) $^{c)}$	$\approx$905, $\approx$765, $\approx$87
α-KDy(WO$_4$)$_2$	$C_{2h}^6 - C2/c$	$^{d)}$	SRS	$\approx$899, $\approx$760
α-KGd(WO$_4$)$_2$	$C_{2h}^6 - C2/c$	Pr^{3+}, Nd^{3+}, Dy^{3+}, Ho^{3+}, Er^{3+}, Tm^{3+}, Yb^{3+}	SRS, self-SRS (Pr^{3+}, Nd^{3+}, Yb^{3+}) $^{c)}$	$\approx$ 901, $\approx$768, $\approx$84
α-KEr(WO$_4$)$_2$	$C_{2h}^6 - C2/c$	Er^{3+}	SRS $^{a)}$	$\approx$905, $\approx$760
α-KLu(WO$_4$)$_2$	$C_{2h}^6 - C2/c$	Pr^{3+}, Nd^{3+}, Ho^{3+}, Er^{3+}, Tm^{3+}, Yb^{3+}	SRS, self-SRS (Nd^{3+}) $^{c)}$	$\approx$907, $\approx$757
CaWO$_4$	$C_{4h}^6 - I4_1/a$	Pr^{3+}, Nd^{3+}, Ho^{3+}, Er^{3+}, Tm^{3+}	SRS	$\approx$908
MnWO$_4$	$C_{2h}^4 - P2/c$	$^{e)}$	**SRS**	**$\approx$879**
ZnWO$_4$	$C_{2h}^4 - P2/c$	Cr^{3+}	SRS $^{f)}$	$\approx$907
RbNd(WO$_4$)$_2$	$C_{2h}^6 - C2/c$	Nd^{3+}	-	-
SrWO$_4$	$C_{4h}^6 - I4_1/a$	Pr^{3+}, Nd^{3+}	SRS, self-SRS (Nd^{3+}) $^{c)}$	$\approx$922
CdWO$_4$	$C_{2h}^4 - P2/c$	$^{e)}$	SRS $^{f)}$	$\approx$890
CsLa(WO$_4$)$_2$	$D_{2d}^4 - P\bar{4}2_1c$	Nd^{3+}	-	-
BaWO$_4$	$C_{4h}^6 - I4_1/a$	Nd^{3+}	SRS, self-SRS (Nd^{3+}) $^{c)}$	$\approx$925, $\approx$332
La$_2$(WO$_4$)$_3$	$C_{2h}^6 - C2/c$	$^{d)}$	SRS	$\approx$940
Gd$_2$(WO$_4$)$_3$	$C_{2h}^6 - C2/c$	Nd^{3+}	-	-
PbWO$_4$	$C_{4h}^6 - I4_1/a$	Nd^{3+}	SRS, self-SRS (Nd^{3+}) $^{c)}$	$\approx$901, $\approx$328

[a)] Unpublished data.
[b)] Space group $S_4^2 - I\bar{4}$ is given by [3].
[c)] Self-SRS, i.e. SRS from the arising SE of Ln^{3+} lasants.
[d)] Some trivalent lanthanide ions Ln^{3+} are possible.
[e)] Some of transition metal and lanthanide ions are possible.
[f)] Can be activated by maser Fe^{3+} and Cr^{3+} ions (see, e.g. [4]).

Table 1 Known SRS- and SE-active tungstate crystals

tural characterization classified MnWO$_4$ to be a member of an isomorphous series AWO$_4$ with A = Mn, Fe, Co, Ni, Zn, Cd, Mg, of which the crystal structure of MgWO$_4$ was described first [6]. A detailed structure determination of MnWO$_4$ with an emphasis on the magnetic order is presented by [7]. The magnetic properties (MnWO$_4$ becomes antiferromagnetic below ca. 14 K) and the magnetic structure have been subject to several detailed investigations. In contrast to the tungstate compounds with Fe, Co, or Ni, which all possess simple antiferromagnetic order with collinear spins at low temperatures, MnWO$_4$ undergoes a series of three phase transitions with complex commensurate and incommensurate (collinear and helicoidal) order of magnetic moments [8–10]. The helicoidal magnetic structure, that occurs in MnWO$_4$ between ca. 12.5 K and ca. 8 K, recently turned out to be a prerequisite of magnetoelectric multiferroic behaviour of MnWO$_4$ [11–13]. Besides investigations of magnetic properties at low temperatures only little information about physical and crystallographic properties of MnWO$_4$ is available in literature [14]. In particular, no information about optical behaviour of the compound is reported.

MnWO$_4$ crystallizes monoclinic with space group $P2/c$ (C_{2h}^4, Nr. 13) [6], its lattice parameters at room temperature are $a = 4.830(1)$ Å, $b = 5.7603(9)$ Å, $c = 4.994(1)$ Å, $\beta = 91.14(2)°$ [14]. The crystal structure consists of alternating zig-zag chains of edge-sharing distorted [MnO$_6$] octahedra and edge-sharing distorted [WO$_6$] octahedra, that run along the c-axis (see Fig. 1). Mn and W atoms occupy positions with site symmetry 2 (C_2), while all oxygen atoms are in general positions with site symmetry 1 (C_1).

Characteristic						
Space group [6]	$C_{2h}^4 - P2/c$ (No. 13) [a]					
Unit cell parameters, Å [14]	$a = 4.830(1)$ $b = 5.7603(9)$ $c = 4.994(1)$ $\beta = 91.14(2)^\circ$					
Formula units per unit cell [6]	$Z = 2$					
Fractional coordinates, site symmetry (ss) and coordination number (CN) of atoms [14]		x	y	z	ss	CN
	Mn:	1/2	0.6856(4)	1/4	$2\,(C_2)$	6
	W:	0	0.1800(1)	1/4	$2\,(C_2)$	6
	O1:	0.211(1)	0.102(1)	0.943(1)	$1\,(C_1)$	
	O2:	0.250(1)	0.374(1)	0.393(1)	$1\,(C_1)$	
Density, g cm^{-3}	$d_x \approx 7.238$					
Melting temperature, K	$T_m \approx 1574$					
Method of crystal growth	flux growth [13,15], floating zone technique [12,13], Czochralski growth [16], top-seeding technique					
Linear optical character	Biaxial positive					
Optical transparency range, μm [b]	≈ 645 nm – > 3500 nm					
Refractive index (modified Sellmeier equation) [c]	$n^2(\lambda) = D_1 + \frac{D_2}{(\lambda^2 - D_3)} - D_4\lambda^2$					
Nonlinearity	$\chi^{(3)}$					
Energy of SRS-promoting vibration mode, cm^{-1}	$\omega_{SRS} \approx 879$					

[a] Paramagnetic room temperature modification. At 13.5 K a modification (“AF3”) with incommensurate magnetic periodicity (propagation vector $\mathbf{k} =$ (-0.214, 1/2, 0.457) occurs with magnetic moments ordered in the *ac*-plane, followed at 12.5 K by a phase with the same incommensurate magnetic periodicity (“AF2”) but with helicoidal ordering of magnetic moments. At 8 K a commensurate magnetic structure (“AF1”) with periodicity ($4a$, $2b$, $2c$) and collinear magnetic ordering in the *ac*-plane is found [8].

[b] For a (010) plate of ≈ 0.5 mm thickness. Transmission limit in the visible wavelength range estimated at 50% of maximum transmission.

[c] Sellmeier coefficients: λ is in μm; (ξ^2 is the sum of the squares of the residuals). The angle between the axis $\mathbf{e}_3$ $(= (1/c)\mathbf{c})$ and the principal axis of the optical indicatrix $\mathbf{e}_3^0$ increases slightly from $\sim 17.8^\circ$ in the visible wavelength range to $\sim 20.0^\circ$ at 2.325 μm (the same angle is found between $\mathbf{e}_1$ and $\mathbf{e}_1^0$, $\mathbf{e}_2$ is parallel to $\mathbf{e}_2^0$).

	D_1	D_2	D_3	D_4	ξ^2
n_1^o	4.685(8)	0.095(11)	0.16(5)	0.0168(13)	1.2×10^{-7}
n_2^o	4.420(24)	0.16(5)	-0.11(16)	0.005(3)	5.2×10^{-7}
n_3^o	5.105(12)	0.107(17)	0.17(6)	0.021(2)	2.6×10^{-7}

Table 2 Crystallographic and some physical properties of monoclinic $MnWO_4$ single crystals at room temperature (Limit of probable error in parentheses)

Stokes and anti-Stokes laser radiation		
Wavelength, μm	Line	SRS- and RFWM-line attribution [a]
0.7744	AS_{t4}	$\omega_f + 4\omega_{SRS}$
0.8310	AS_{t3}	$\omega_f + 3\omega_{SRS}$
0.8966	AS_{t2}	$\omega_f + 2\omega_{SRS}$
0.9731	AS_{t1}	$\omega_f + \omega_{SRS}$
1.06415	λ_f	ω_f
1.1740	S_{t1}	$\omega_f - \omega_{SRS}$
1.3091	S_{t2}	$\omega_f - 2\omega_{SRS}$
1.4793	S_{t3}	$\omega_f - 3\omega_{SRS}$

[a] $\omega_{SRS} \approx 879$ cm^{-1}.

Table 3 Spectral composition of $\chi^{(3)}$ nonlinear lasing (at room-temperature) in a monoclinic single crystal of $MnWO_4$ with Nd^{3+}:$Y_3Al_5O_{12}$ picosecond laser pumping at $\lambda_f = 1.06415$ μm wavelength (Excitation geometry $e_3(e_1e_1)e_3$)

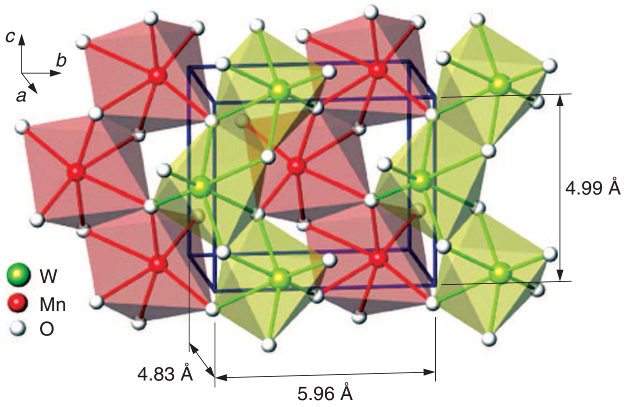

Figure 1 (online color at www.lphys.org) Section of the crystal structure of $MnWO_4$. The sixfold coordination of both, Mn and W, by oxygen is indicated by coordination polyhedra marked in green for $[MnO_6]$ and in red for $[WO_6]$. The unit cell of the structure is indicated

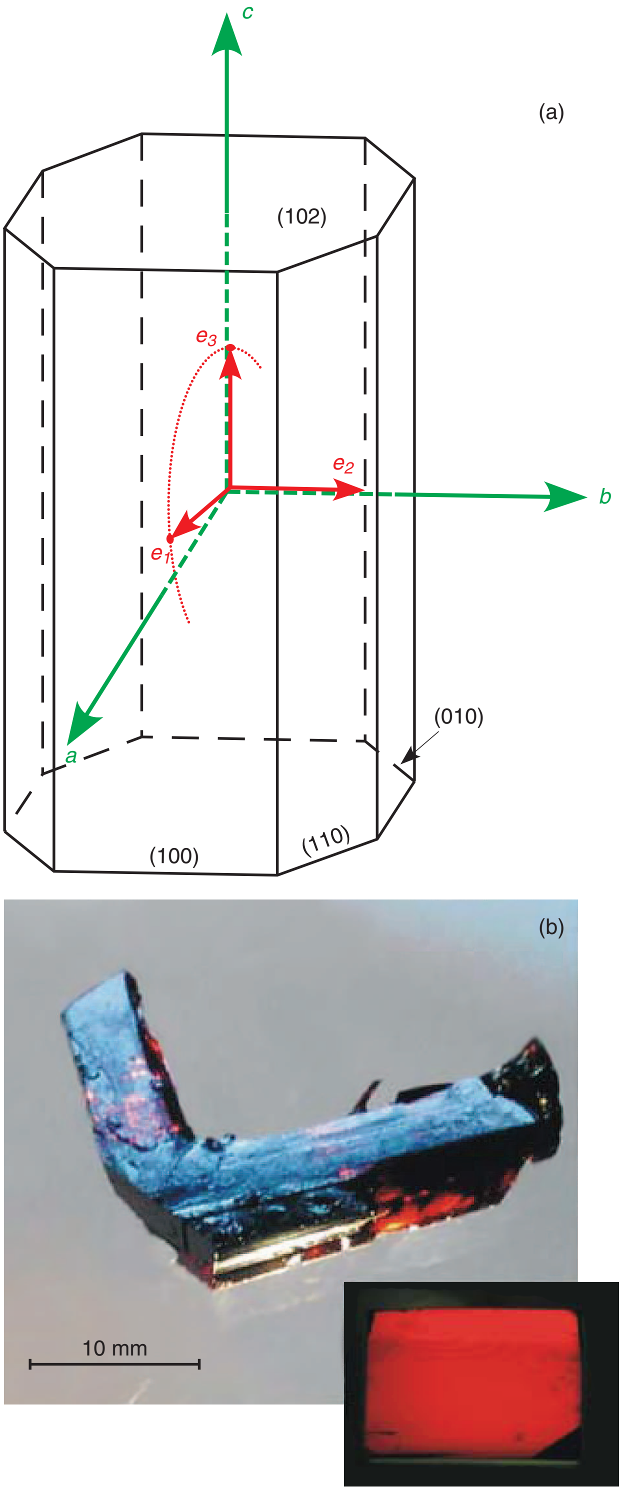

Figure 2 (online color at www.lphys.org) (a) Typical morphology of grown $MnWO_4$ crystals with face indices. Crystallographic axes **a**, **b**, **c** and axes of the Cartesian reference system $\mathbf{e}_1$, $\mathbf{e}_2$, $\mathbf{e}_3$ are indicated. (b) Example of a grown crystal of $MnWO_4$; the inset shows the sample used for our measurements in transmitted light with crossed polarizers (dimensions 3.94×2.73 mm^2, see also text)

During the single crystal growth process of $MnWO_4$ special care was taken to keep manganese in divalent state. Using the flux technique and (based on early work of [15]) a melt solvent of the system Na_2WO_4-WO_3 we found that all crystals grown by this method were dark brown/black as bulk crystals and brown in thin section, indicating that manganese is not purely divalent. By the use of high growth temperatures and the renouncement of melt solvents this problem could be eliminated. DTA analysis proved that $MnWO_4$ melts congruently at ~ 1574 K, the compound is slightly volatile at this temperature. By application of the top seeded growth technique and low cooling rate (2 K within 24 h) ruby-red transparent single crystals with dimensions up to $5 \times 5 \times 25$ mm^3 were obtained; an example is presented in Fig. 2b. Typically, the crystals are elongated along the c-axis and bounded by (100), (110), (010), and (102), see Fig. 2a, occasionally also faces (011) are found instead of (102). The crystals show a pronounced cleavage parallel (010). Refractive indices were determined in the wavelength range from 0.852 to 2.325 μm at six discrete wavelengths using the prism method and two polished prisms with face of incidence (100) and (010), respectively. The experimental data were fitted with a modified Sellmeier equation (see Table 2), the results are given in Table 2 and presented, together with a transmission spectrum, in Fig. 3. For our SRS investigations a sample (rectangular parallel-epiped with dimensions $2.94 \times 2.73 \times 3.94$ mm^3) with face normals parallel to $\mathbf{e}_3$ $(= (1/c)\,\mathbf{c})$, $\mathbf{e}_2$ $(= (1/b)\,\mathbf{b})$, and $\mathbf{e}_1$ $(= \mathbf{e}_2 \times \mathbf{e}_3)$, respectively, was used. All faces were polished but without anti-reflection coating. Some physical properties of $MnWO_4$ single crystals at room temperature are listed in Table 2.

3. Stokes and anti-Stokes generation

According to the limited transmission of $MnWO_4$ in the visible wavelength range (see Fig. 3), single-pass Raman induced Stokes and anti-Stokes generation was excited at a fundamental wavelength $\lambda_f = 1.06415$ μm using a home-made Xe-flashlamp–pumped picosecond ($\tau_p \approx 100$ ps) Nd^{3+}:$Y_3Al_5O_{12}$ laser. The nearly Gaussian profile pumping beam was focused into the sample with a lens ($f = 25$ cm), resulting in beam-waist diameter of about 160 μm. An excitation geometry $e_3(e_1e_1)e_3$, i.e. incident laser beam along $\mathbf{e}_3$ with polarization direction parallel $\mathbf{e}_1$, generated wave along $\mathbf{e}_3$ with polarization direction parallel $\mathbf{e}_1$, was applied. The spectral composition of the SRS and Raman induced four-wave mixing (RFWM) lasing components was analysed with a grating monochromator (McPherson Model 270 in Czerny-Turner arrangement) and recorded by a spectrometric system (CSMA) equipped with two Hamamatsu linear image sensors (Si-CCD (3923-1024Q) with maximum sensitivity around 0.65 μm and InGaAs-CCD (G9204-512D) offering good sensitivity from 0.9 till 1.7 μm spectral region). Obtained Stokes and anti-Stokes components are shown in Fig. 4 and summarized in Table 3.

Due to the essentially steady-state (ss) pumping condition $\tau_p \gg T_2 = (\pi \Delta\nu_R)^{-1} \approx 1.5$ ps (here, T_2 and $\Delta\nu_R$ are the phonon dephasing time and the linewidth of the Raman transition, respectively) for the $MnWO_4$ crystal in our SRS experiments we can estimate the Raman gain coefficient g_{ssR}^{St1} for its first Stokes lasing component at $\lambda_{St1} = 1.1740$ μm. This was done by the comparative measurement of the "threshold" pump intensities I_p^{thr} (I_p^{thr} according to the conventional definition adopted in [17]) of our $MnWO_4$ sample and of a reference tungstate crystal ($PbWO_4$, see [18]) with known g_{ssR}^{St1} value ($\approx$3.1 cm GW^{-1} for λ_{St1} =1.1770 cm^{-1} [19]). To derive the Raman gain coefficient of $MnWO_4$ from these measurements we applied the sufficiently tested method based on the well-known relation $g_{ssR}^{St1} I_p^{thr} l_{SRS} \approx 30$ [20]. The measurement of the "threshold" pump intensity necessary for an unambiguous observation of the first Stokes for both tungstate crystals (for $MnWO_4$ along the c-axis and for $PbWO_4$ perpendicular to the c-axis) with similar SRS-active length (l_{SRS}) showed that for $PbWO_4$ I_p^{thr} is more than two times that of $MnWO_4$. Consequently, the steady-state Raman gain coefficient g_{ssR}^{St1} for $MnWO_4$ is not less than 6.2 cm GW^{-1}.

For crystals with wolframite-type structure of symmetry $P2/c$ with two formula units per primitive cell, particularly for $MnWO_4$ as well as for the two isostructural SRS-active tungstates $ZnWO_4$ and $CdWO_4$ [18], a factor group analysis (see e.g. [21]) shows that the number of degrees of freedom is $3NZ = 36$, that gives the following set of irreducible representations for all vibration modes (in Brillouin-zone center at $\mathbf{k} = 0$): $\Gamma_{36} = 8A_g + 10B_g + 8A_u + 10B_u$. Among them the $(8A_g + 10B_g)$ modes are the Raman active vibrations, $(A_u + 2B_u)$ are the acoustic modes, and the remaining $(7A_u + 8B_u)$ modes are IR-active vibrations. Taking into consideration the numerous reported investigations of Raman spectra of crystals with wolframite-type structure (see e.g. [22]) it can be concluded that the SRS-promoting phonon mode with frequency $\omega_{SRS} \approx 879$ cm^{-1} that was observed for $MnWO_4$ in our investigations corresponds to the A_g (W-O) stretching vibration of the WO_6 groups.

4. Conclusion

We have discovered the $\chi^{(3)}$ nonlinear optical potential for monoclinic $MnWO_4$ crystals as a high-gain Raman material for laser frequency converters in the near- and mid-IR spectral ranges. Due to the multiferroic nature of $MnWO_4$ at cryogenic temperatures there could be possibly some optical phenomena that may be influenced by applied magnetic or electric field. We also hope that this tungstate could also be a host material for lanthanide and transition-metal lasant ions.

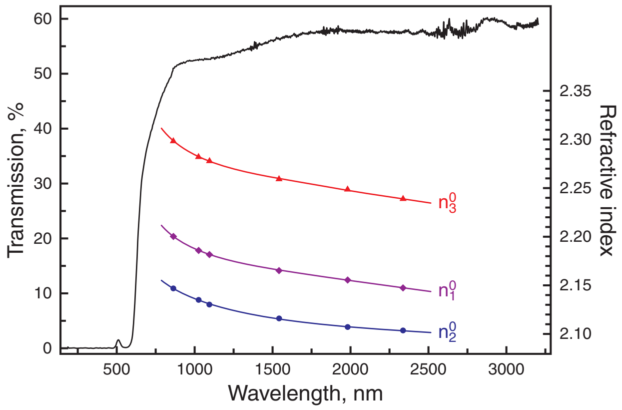

Figure 3 (online color at www.lphys.org) Room-temperature transmission spectrum in the range from the visible to mid-IR and wavelength dispersion of refractive indices for the wavelength range from 0.852 μm to 2.325 μm of monoclinic $MnWO_4$. Symbols represent measured data, connecting lines are the graphs of the respective Sellmeier fits

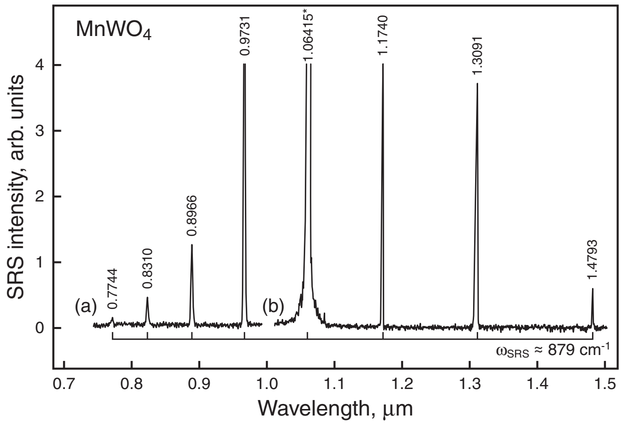

Figure 4 Room-temperature SRS and RFWM spectra of a monoclinic $MnWO_4$ single crystal recorded in pumping geometry $e_3(e_1e_1)e_3$ (see text) under laser excitation at $\lambda_f = 1.06415$ μm wavelength (marked by an asterisk). Wavelength of all lines given in μm, and their intensity are shown without correction for the spectral sensitivity of the analysing CSMA system with Si-CCD (a) and GaInAs-CCD (b) sensors. Stokes and anti-Stokes lines related to the SRS-promoting vibration mode of the crystal $\omega_{SRS} \approx 879$ cm^{-1} are indicated by horizontal brackets

Acknowledgements The research reported here was performed within the "Joint Open Laboratory for Laser Crystals and Precise Laser Systems" and supported in part by the Russian Foundation for Basic Research and the program of the Presidium of Russian Academy of Sciences "Femtosecond optics and new optical materials", as well as by the Deutsche Forschungsgemeinschaft under sign SFB 608, the University of Cologne and the Technical University of Berlin. One of us (A.A.K.) is grateful also to the

Alexander von Humboldt Foundation for the "Festkörperphysik" Research Prize, which allowed him to carry out SRS experiments at the Institute of Optics and Atomic Physics of the Technical University of Berlin.

References

[1] A.A. Kaminskii, Crystalline Lasers: Processes and Operating Schemes (CRC Press, Boca Raton, FL, 1996); M.J. Weber, Handbook of Laser Wavelengths (CRC Press, Boca Raton, FL, 2000).
[2] L.F. Johnson and K. Nassau, Proc. IRE **49**, 1704 (1961).
[3] J. Hanuza, A. Haznar, M. Maczka, A. Pietraszko, A. Lemiec, J.H. van der Maas, and E.T.G. Lutz, J. Raman Spectrosc. **28**, 953 (1997).
[4] L.G. Van Uitert and S. Preziosi, J. Appl. Phys. **33**, 2908 (1962).
[5] C. Palache, H. Berman, and C. Frondel (eds.), The System of Mineralogy, Vol. II, (Wiley, New York, 1951), p. 1064.
[6] E.K. Broch, in: C. Hermann, O. Lohrmann, and H. Philipp (eds.), Strukturberichte II, 1928–1932 (Akademische Verlagsgesellschaft M.B.H., Leipzig, 1937), p. 450.
[7] H. Dachs, E. Stoll, and H. Weitzel, Z. Kristallogr. **125**, 120 (1967).
[8] G. Lautenschläger, H. Weitzel, T. Vogt, R. Hock, A. Böhm, M. Bonnet, and H. Fuess, Phys. Rev. B. **48,** 6087 (1993).
[9] H. Ehrenberg, H. Weitzel, C. Heid, H. Fuess, G. Wltschek, T. Kroener, J. van Tol, and M. Bonnet, J. Phys.: Condens. Matter **9**, 3189 (1997).
[10] H. Ehrenberg, H. Weitzel, H. Fuess, and B. Hennion, J. Phys.: Condens. Matter **11**, 2649 (1999).
[11] O. Heyer, N. Hollmann, I. Klassen, S. Jodlauk, L. Bohatý, P. Becker, J.A. Mydosh, T. Lorenz, and D. Khomskii, J. Phys.: Condens. Matter **18**, L471 (2006).
[12] K. Taniguchi, N. Abe, T. Takenobu, Y. Iwasa, and T. Arima, Phys. Rev. Lett. **97**, 097203 (2006).
[13] A.H. Arkenbout, T.T.M. Palstra, T. Siegrist, and T. Kimura, Phys. Rev. B **74**, 184431 (2006).
[14] J. Macavei and H. Schulz, Z. Kristallogr. **207**, 193 (1993).
[15] D. Schultze, K.-Th. Wilke, and Ch. Waligora, Z. Anorg. Allg. Chemie **352**, 184 (1967).
[16] L.G. van Uitert, J.J. Rubin, and W.A. Bonner, J. Am. Ceram. Soc. **46**, 512 (1963).
[17] M. Klein, M. Maier, and W. Prettl, Phys. Rev. B **28**, 6008 (1983); K.K. Lai, W. Schüsslbauer, H. Silberbauer, H. Amler, U. Bogner, M. Maier, M. Jordan, and H.-J. Jodl, Phys. Rev. B **42**, 5834 (1990); A.A. Kaminskii, E. Haussühl, J. Hulliger, K. Ueda, K. Takaichi, J. Hanuza, H.J. Eichler, and G.M.A. Gad, Phys. Stat. Sol. (a) **193**, 167 (2002); A.A. Kaminskii, P. Becker, L. Bohatý, K. Ueda, K. Takaichi, J. Hanuza, M. Maczka, H.J. Eichler, and G.M.A. Gad, Opt. Commun. **206**, 179 (2002).
[18] A.A. Kaminskii, H.J. Eichler, K. Ueda, N.V. Klassen, B.S. Redkin, L.E. Li, J. Findeisen, D. Jaque, J. García-Sole, J. Fernández, and R. Balda, Appl. Optics **38**, 4533 (1999).
[19] A.A. Kaminskii, C.L. McCray, H.R. Lee, S.W. Lee, D.A. Temple, T.H. Chyba, W.D. Marsh, J.C. Barnes, A.N. Annanenkov, V.D. Legun, H.J. Eichler, G.M.A. Gad, and K. Ueda, Opt. Commun. **183**, 277 (2000).
[20] W. Kaiser and M. Maier, in: F.T. Arichi and E.O. Schultz-Dubois (eds.), Laser Handbook, Vol. 2 (North-Holland, Amsterdam, 1972), p. 1077; Y.R. Shen, The Principles of Nonlinear Optics (Wiley, New York, 1984).
[21] D.L. Rousseau, R.P. Bauman, and S.P.S. Porto, J. Raman Spectrosc. **10**, 253 (1981).
[22] J.P. Lesne and P. Caillet, Canadian J. Spectrosc. **18**, 69 (1973); G. Blasse, J. Inorg. Nucl. Chem. **37**, 97 (1975); Y. Liu, H. Wang, G. Chen, Y.D. Zhou, B.Y. Gu, and B.Q. Hu, J. Appl. Phys. **64**, 4651 (1988); M. Mączka, J. Hanuza, A.F. Fuentes, and U. Amador, J. Raman Spectrosc. **33**, 56 (2002); A. Jayaraman, S.Y. Wang, and S.K. Sharma, Phys. Rev. B **52**, 9886 (1995).